



POLITECNICO
MILANO 1863

SCUOLA DI INGEGNERIA INDUSTRIALE
E DELL'INFORMAZIONE

EXECUTIVE SUMMARY OF THE THESIS

Kinematic and Kinetic Outcomes of Different Tibiofemoral Component Size Combinations in Total Knee Arthroplasty: A Musculoskeletal Modelling Study

LAUREA MAGISTRALE IN BIOMEDICAL ENGINEERING - INGEGNERIA BIOMEDICA

Author: EVA CUKO

Advisor: PROF. TOMASO MARIA TOBIA VILLA

Co-advisors: PROF. WILLIAM R. TAYLOR, DR. SEYYED HAMED HOSSEINI NASAB

Academic year: 2025-2026

1. Introduction

Total Knee Arthroplasty (TKA) is the gold-standard surgical treatment for patients with end-stage osteoarthritis, effectively reducing pain and restoring knee function. Osteoarthritis is the most prevalent musculoskeletal disorder worldwide, and its incidence is expected to rise substantially in the coming decades, driving a corresponding increase in TKA procedures. Despite the overall success of TKA, a notable proportion of patients report postoperative dissatisfaction, sometimes necessitating complex and costly revision surgeries. Among the factors influencing postoperative outcomes, tibiofemoral component size combinations have been suggested as a potential contributor to revision risk. Surgeons frequently combine different femoral and tibial sizes to optimize anatomical fit, yet the biomechanical consequences of these combinations remain poorly understood. Previous studies have primarily relied on *in vitro* experiments [1] or finite element (FE) analyses, which focus on implant mechanics and provide limited insight into joint-level kinematics during functional activities. This study employs musculoskeletal (MSK) modelling

to investigate how different tibiofemoral component size combinations of the Columbus DD total knee prosthesis (Aesculap) affect knee kinematics and kinetics during walking and squatting. MSK models enable dynamic, subject-specific predictions of joint loads and motions [2], offering a comprehensive assessment of knee biomechanics that overcomes typical limitations of *in vivo* and *in vitro* methods. The findings of this study may help inform surgical planning, improve clinical outcomes, and provide useful insights for manufacturers.

2. Materials & Methods

2.1. Experimental data & K5R model

A previously validated subject-specific lower limb musculoskeletal model of a TKA patient with a cruciate-sacrificing Innex FIXUC implant (Zimmer Biomet) was used as the starting point [2]. The model represented subject K5R (65 years, 1.74 m, 95.6 kg) from the CAMS-Knee dataset [3], which provides tibiofemoral kinematics and *in vivo* knee contact forces. Only level walking and squatting were analyzed, with five motion cycles per task. The model included subject-

specific bone geometries reconstructed from CT images, 44 muscles on the right leg, and major knee ligaments represented by nonlinear springs. Tibiofemoral and patellofemoral kinematics were modeled using 3D implant meshes and elastic foundation contact mechanics [4].

2.2. Columbus DD baseline model: Modeling Pipeline 1

To analyze different tibiofemoral size combinations of the posterior cruciate-retaining Columbus DD (Columbus Deep Dish, Aesculap, Tuttlingen, Germany), a new musculoskeletal model was created. Implant CAD geometries for the matched size combination (F4T4) were preprocessed and aligned with the reference Innex FIXUC geometry of the K5R base model to preserve anatomical correspondence. The aligned meshes were integrated into the base musculoskeletal model, maintaining its structural hierarchy. This model served as the baseline Columbus DD configuration and as the reference for generating additional tibiofemoral size combinations.

2.3. Simulation Workflow

All simulations were carried out using the Concurrent Optimization of Muscle Activations and Kinematics (COMAK) framework within OpenSim, with model creation and simulation management performed in MATLAB. Primary joint coordinates (angles, velocities, accelerations) were first computed with COMAK Inverse Kinematic [2] and, together with ground reaction forces, COMAK algorithm predicted secondary tibiofemoral and patellofemoral DoFs, muscle activations, ligament, and knee contact forces by minimizing a muscle redundancy cost function (Eq. 1) [4]. Joint contact forces and pressures were subsequently computed using the Joint Mechanics tool.

$$\min \sum_{i=1}^{n_{\text{muscles}}} V_i (a_i)^2 \quad (1)$$

Eq. 2.1: Cost function minimized by COMAK, defined as the sum of squared muscle activations $(a_i)^2$ weighted according to muscle volume V_i .

2.4. Columbus DD baseline model Verification

For the Columbus DD baseline model, five gait and five squat cycles were simulated and

qualitatively compared with *in vivo* CAMS-Knee data. Ranges of motion, temporal trends, and peak timings of tibiofemoral kinematics (flexion–extension, adduction–abduction, internal–external rotation, translations) and kinetics (contact forces and moments) were visually inspected to assess physiological plausibility. The cycle best matching *in vivo* data was selected as the representative baseline (walking cycle 1, squatting cycle 3) and used for subsequent analysis.

2.5. Size Combinations MSK Models: Modeling Pipeline 2

Alternative tibiofemoral size combinations were defined based on clinically relevant deviations of one or two sizes. Femoral oversizing was simulated by increasing the femoral component by one (F5T4) and two sizes (F6T4), while tibial undersizing was simulated by decreasing the tibial component by one (F4T3) and two sizes (F4T2). Implant geometries for each configuration were integrated into the baseline Columbus DD model, and walking (cycle 1) and squatting (cycle 3) simulations were performed to obtain kinematic and kinetic outputs.

2.6. Comparison of the results

To evaluate the effects of tibiofemoral size variations, outputs from each model were compared with the Columbus DD baseline (F4T4). Kinematic and kinetic curves were visually inspected and deviations quantified using root mean square errors (RMSE). Size combinations with the largest RMSE were further analyzed for peak differences relative to baseline. For walking, analysis focused on adduction–abduction, internal–external rotation, and anterior–posterior translation, based on their sensitivity to size variations and relevance for the activity, while flexion–extension and medial–lateral translations were excluded due to task-driven motion and noise sensitivity, respectively. For squatting, the same rationale was applied, with the addition of proximal–distal translation due to its relevance for the activity. Kinetic outcomes comprised medial, lateral, and total contact forces, as well as mean medial and lateral contact pressures. As simulations were deterministic and based on a single subject, interpretation relied on direct comparison without statistical analysis.

3. Results

3.1. Baseline Model Verification

For level walking and squatting, the representative baseline cycles (walking cycle 1, squatting cycle 3) showed the highest agreement with *in vivo* measurements. Peak total contact forces reached approximately 3.0 BW (walking) and 4.0 BW (squatting). Secondary kinematics ranged as follows: adduction-abduction -1° to 2° (walking) and -1° to 1° (squatting); internal-external rotation -10° to 5° (walking) and -10° to -2° (squatting); anterior translation -10 to 5 mm (walking) and -8 to -1 mm (squatting); superior translation 19 – 22 mm (walking) and 19 – 24 mm (squatting).

3.2. Size Combinations Results

3.2.1 Walking Kinematics

During level walking, all tibiofemoral size combinations exhibited patterns largely consistent with the baseline configuration (F4T4)(Fig. 1). The analysis focused on the following three DoFs: adduction–abduction, internal–external rotation, and anterior–posterior (AP) translation. During the loading response phase (0–10% of the gait cycle), all configurations showed knee abduction–adduction near 0° and minor deviations in internal–external rotation, with larger femoral components (F5T4, F6T4) slightly reducing external rotation and smaller tibial components (F4T2, F4T3) closely matching baseline. AP translation was posterior for all combinations, reflecting near-full knee extension at heel strike. Size-dependent differences were most pronounced from mid-stance to pre-swing (10–60%). Larger femoral components exhibited increased adduction (F6T4 average RMSE 0.22° , peak -0.35°), while smaller tibial components showed slightly reduced adduction. External–internal rotation was preserved overall, except for F4T2, which showed increased external rotation (average RMSE 0.59° , peak -2.01°). AP translation shifted posteriorly for smaller tibial components, whereas larger femoral components remained near or slightly anterior to baseline. F6T4 showed the largest deviations during swing, with average RMSE 1.5 mm and peak differences up to 1.6 mm.

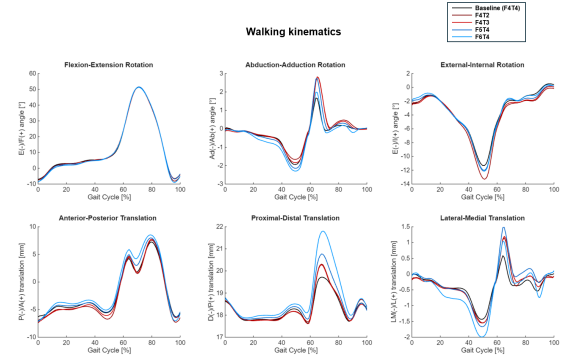


Figure 1: Walking kinematics of all tibiofemoral size combinations showing six DoFs.

3.2.2 Squatting Kinematics

During the squat cycle, all size combinations followed the general baseline kinematic trends, with smaller tibial components (F4T2, F4T3) showing minimal deviations and larger femoral components (F5T4, F6T4) exhibiting greater deviations (Fig. 2). The analysis focused on the following four DoFs: adduction–abduction, internal–external rotation, anterior–posterior and proximal–distal translations. Smaller tibial components closely matched baseline across all DoFs. Larger femoral components increased adduction (F6T4 RMSE 0.36° , peak -0.35° during deep flexion) and reduced external rotation (F6T4 RMSE 0.93° , peak 1.23°). AP translation showed increased anterior shift for larger femoral components, with F6T4 reaching RMSE 2.1 mm and peak differences of 2.7 mm in both descent and ascent phases. Proximal–distal translation was largely unchanged for smaller tibial components, while F6T4 exhibited the greatest deviation (RMSE 2.68 mm, peak 4.63 mm at deep flexion).

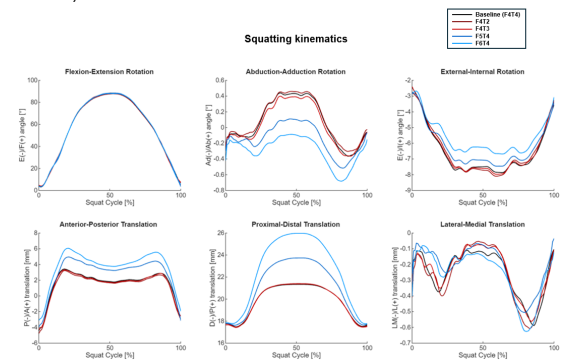


Figure 2: Squatting kinematics of all tibiofemoral size combinations showing six DoFs.

3.2.3 Walking Kinetics

Medial, lateral, and total tibiofemoral contact forces generally followed baseline patterns across all size combinations (Fig. 3). F6T4 consistently exhibited the largest deviations, with medial peak differences of -0.012 BW, lateral peak differences of 0.18 BW, and total contact force peak differences of -0.083 BW during pre-swing. Smaller tibial components (F4T2) showed minor variations relative to baseline.

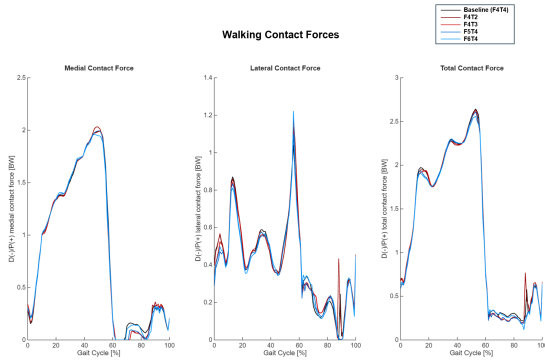


Figure 3: Walking tibiofemoral contact forces for all size combinations.

Medial and lateral mean contact pressures also tracked baseline trends (baseline peaks: 13 MPa medial, 23 MPa lateral)(Fig. 4), with larger femoral components reducing medial pressures (F6T4 mean RMSE 2.53 MPa, peak difference 3.0 MPa) and smaller tibial components closely following baseline. Lateral pressures showed more pronounced deviations in mid-stance to pre-swing, with F4T2 exhibiting the largest peak error (8.15 MPa).

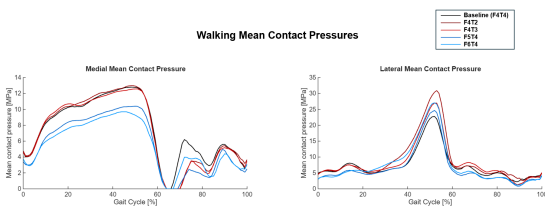


Figure 4: Walking tibiofemoral mean contact pressures for all size combinations.

At the second peak of total contact force (53% gait cycle), medial pressures were concentrated in the mid-contact region of the tibial inlay, with F6T4 showing the lowest value (21.3 MPa) and baseline the highest (27.9 MPa)(Fig. 5). Lateral pressures peaked at the posterior edge of the tibia inlay, with F4T2 exhibiting the maximum contact pressure (69.7 MPa) among all combinations, exceeding the baseline (50.4 MPa).

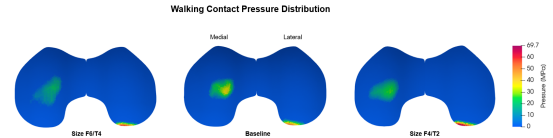


Figure 5: Contact pressure distribution at second peak of total contact force.

3.2.4 Squatting Kinetics

Medial, lateral, and total tibiofemoral contact forces generally followed baseline patterns across all size combinations, with minor deviations primarily in the central phase of the squat cycle (Fig. 6). F4T2 showed the largest medial deviation (RMSE 0.036 BW, peak -0.07 BW), while F6T4 exhibited the largest lateral deviation (RMSE 0.15 BW, peak -0.30 BW) and the greatest reduction in total contact force (RMSE 0.15 BW, peak -0.32 BW).

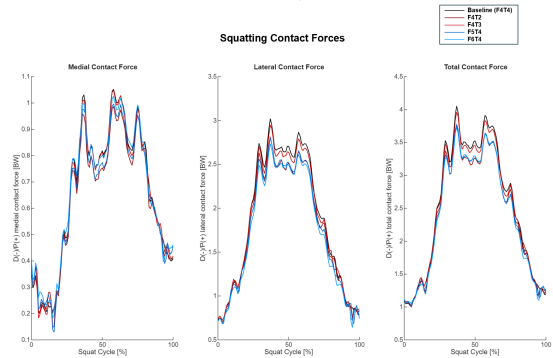


Figure 6: Squatting tibiofemoral contact forces for all size combinations.

Medial and lateral mean contact pressures were generally lower than baseline (baseline peaks: 17 MPa medial, 29 MPa lateral)(Fig. 7). Contact pressures were most affected by larger femoral components. For medial contact, F5T4 showed the largest deviation (RMSE 3 MPa, peak -4.8 MPa), while for lateral contact, F5T4 exhibited an RMSE of 4.52 MPa and peak -6.3 MPa, and F6T4 reached the highest local RMSE of 6.6 MPa during deep knee flexion (45 – 65% of the squat cycle).

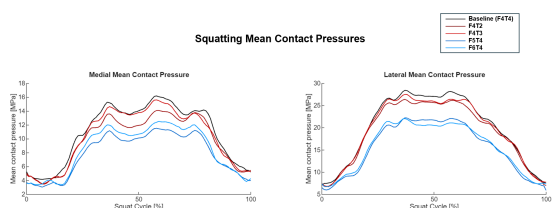


Figure 7: Squatting tibiofemoral mean contact pressures for all size combinations.

At the largest knee flexion angle (88°), tibiofemoral contact pressure distribution was primarily located in the mid-contact region of the tibial inlay, with the lateral compartment slightly posterior (Fig. 8). Notably, the baseline configuration exhibited the highest maximum pressures in both compartments (Medial = 28.3 MPa, Lateral = 51.8 MPa).

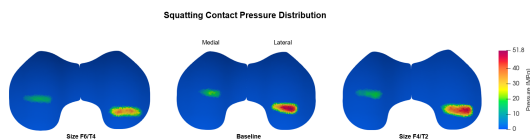


Figure 8: Contact pressure distribution at the largest knee flexion angle (88°).

4. Discussion

4.1. Baseline model verification

The selected baseline cycles closely followed the overall trends and peak timings of *in vivo* CAMS-Knee measurements for both walking and squatting, with minor differences in magnitude and signal offsets, as expected due to geometric differences between the two implant designs (*in silico* Columbus DD vs. *in vivo* Innex FIXUC). Kinematic and kinetic values remained within CAMS-Knee ranges [3] and were consistent with other musculoskeletal modeling studies of TKA [5], supporting their use as a physiologically plausible baseline for evaluating different size combinations.

4.2. Walking Main Findings

Tibiofemoral component sizing had minimal impact on knee kinematics in a Columbus DD prosthesis knee. During level walking, all size combinations closely followed the baseline, with RMSE below 0.6° for abduction–adduction and internal–external rotations, and below 1.5 mm for anterior–posterior translation. Two-size mismatches (F6T4, F4T2) showed the greatest deviations, yet these remained small relative to physiological ranges and are unlikely to affect joint stability or functional mobility. Kinetics were similarly preserved: medial, lateral, and total contact forces closely matched baseline patterns (total contact force RMSE = 0.03 BW), indicating that moderate mismatches up to two sizes do not substantially alter global joint mechanics. Contact pressures were more sensitive to component size. The larger femoral component (F6T4)

slightly reduced medial mean pressures (RMSE 2.5 MPa), while the smaller tibial component (F4T2) showed elevated lateral peak pressures (mean up to 8.15 MPa, maximum 69.7 MPa at the posterior tibial edge), likely due to slightly increased external rotation and posterior tibial translation, combined with differences in contact area and surface conformity. These elevated peaks in F4T2 could be mechanically relevant under repetitive loading, potentially contributing to polyethylene wear, edge delamination, or fatigue damage, whereas the medial compartment remained more centrally loaded, highlighting that stress alterations are highly compartment- and configuration-dependent.

4.3. Squatting Main Findings

During squatting, all size combinations preserved the overall kinematic pattern of the baseline, with deviations larger than in walking, especially in deep flexion (45–65% of the cycle). Larger femoral components showed slightly greater deviations, while smaller tibial components remained closer to baseline. Overall deviations were minimal (RMSE below 0.93° for abduction–adduction and internal–external rotation, up to 2.1 mm anterior–posterior, 2.68 mm proximal–distal), remaining small relative to physiological ranges and unlikely to affect joint stability or functional mobility. Squatting kinetics closely followed baseline patterns. Even in two-size mismatch configurations (F4T2, F6T4), total contact force deviations were moderate (RMSE up to 0.15 BW; peak difference -0.32 BW), with larger femoral components associated with slightly reduced lateral and total contact forces. These results indicate that moderate mismatches up to two sizes do not substantially alter global joint mechanics. Contact pressures were more sensitive to component size. Larger femoral components reduced medial and lateral mean pressures (medial RMSE up to 3 MPa; lateral RMSE up to 4.52 MPa), while smaller tibial components remained near baseline. These reductions likely reflect variations in surface conformity, which modify engagement between femoral condyles and the tibial inlay, redistributing load over a broader area. The baseline configuration exhibited the highest pressures; despite being considered the nominal configuration, it does not necessarily represent the most mechanically favorable con-

dition during deep flexion, as local pressures are strongly influenced by surface conformity and engagement patterns across size combinations.

4.4. Comparison with Literature and Clinical Implications

The results show that tibiofemoral size variations of up to two sizes in the Columbus DD system do not substantially affect knee kinematics or joint contact loads during walking and squatting. This aligns with *in vitro* findings [1], which attribute preserved squatting kinematics to the high congruency of the design across size combinations. Clinically, these results support using femoral and tibial components differing by one or two sizes without compromising knee biomechanics. Variability in literature outcomes may reflect differences in TKA system congruency and design, highlighting the importance of documenting these factors when interpreting revision rates and clinical results.

4.5. Limitations and Outlooks

This study has several limitations. First, contact pressures may partly reflect constraints of the elastic foundation model [4], which estimates pressures based on surface proximity and may overestimate peaks at contact boundaries. Integrating musculoskeletal simulations with finite element analyses [5] using subject-specific kinetics could provide more accurate pressure predictions. Second, the study is based on a single subject-specific model, with one walking and one squatting cycle and a single prosthesis design, limiting generalizability of results. While all MSK models preserved baseline structure and alignment, mesh definition, particularly in complex geometries, remains a sensitivity factor affecting convergence and may benefit from further optimization. Additionally, the patellar position within the models could be further refined according to femoral component size. Baseline verification against *in vivo* Innex FIXUC data was qualitative; however, physiological plausibility was confirmed, and consistent modeling across size combinations ensures reliable comparative analysis. Finally, only prosthetic sizing was varied deterministically, whereas knee biomechanics are influenced by multiple interacting factors, including soft tissue behavior, warranting further investigation to fully capture the biomechanical

effects of component size variations.

5. Conclusions

Using tibiofemoral size combinations differing by up to two sizes did not substantially affect knee kinematics or contact loads during walking and squatting, supporting the safe use by surgeons of different tibiofemoral size combinations within the Columbus DD system. Contact pressures were most sensitive to component sizing: localized variations in contact pressure were observed, which could potentially affect implant longevity (e.g., wear or edge delamination), and these effects warrant further investigation to assess their dependence on the specific size combinations used. Overall, this feasibility study provides a good starting point for future research on how tibiofemoral size combinations affect prosthetic knee biomechanics.

References

- [1] I. Dupraz et al. Impact of femoro-tibial size combinations and tka design on kinematics. *Arch. Orthop. Trauma Surg.*, 142 (6):1197–1212, June 2022. doi: 10.1007/s00402-021-03923-y.
- [2] N. Guo et al. Posterior tibial slope influences joint mechanics and soft tissue loading after total knee arthroplasty. *Front. Bioeng. Biotechnol.*, 12:1352794, April 2024. doi: 10.3389/fbioe.2024.1352794.
- [3] W. R. Taylor and et al. A comprehensive assessment of the musculoskeletal system: The cams-knee data set. *J. Biomech.*, 65:32–39, December 2017. doi: 10.1016/j.jbiomech.2017.09.022.
- [4] M. Febrer-Nafría, M. J. Dreyer, A. Maas, W. R. Taylor, C. R. Smith, and S. H. Hosseini Nasab. Knee kinematics are primarily determined by implant alignment but knee kinetics are mainly influenced by muscle coordination strategy. *J. Biomech.*, 161:111851, December 2023. doi: 10.1016/j.jbiomech.2023.111851.
- [5] C. Curreli, F. Di Puccio, G. Davico, L. Modenese, and M. Viceconti. Using musculoskeletal models to estimate in vivo total knee replacement kinematics and loads: Effect of differences between models. *Front. Bioeng. Biotechnol.*, 9:703508, July 2021. doi: 10.3389/fbioe.2021.703508.